Review article

Check for updates

Quantum sensors for biomedical applications

Nabeel Aslam[1,2,3], Hengyun Zhou[1], Elana K. Urbach[1], Matthew J. Turner[4,5], Ronald L. Walsworth[4,5,6], Mikhail D. Lukin[1] & Hongkun Park [1,2] ✉

Abstract

Quantum sensors are finding their way from laboratories to the real world, as witnessed by the increasing number of start-ups in this field. The atomic length scale of quantum sensors and their coherence properties enable unprecedented spatial resolution and sensitivity. Biomedical applications could benefit from these quantum technologies, but it is often difficult to evaluate the potential impact of the techniques. This Review sheds light on these questions, presenting the status of quantum sensing applications and discussing their path towards commercialization. The focus is on two promising quantum sensing platforms: optically pumped atomic magnetometers, and nitrogen–vacancy centres in diamond. The broad spectrum of biomedical applications is highlighted by four case studies ranging from brain imaging to single-cell spectroscopy.

Sections

[1]Department of Physics, Harvard University, Cambridge, MA, USA. [2]Department of Chemistry and Chemical Biology, Harvard University, Cambridge, MA, USA. [3]Institute of Condensed Matter Physics, Technische Universität Braunschweig, Braunschweig, Germany. [4]Quantum Technology Center, University of Maryland, College Park, MD, USA. [5]Department of Electrical and Computer Engineering, University of Maryland, College Park, MD, USA. [6]Department of Physics, University of Maryland, College Park, MD, USA. ✉e-mail: hpark@g.harvard.edu

Review article

Key points

- Quantum sensors can detect magnetic fields and other physical quantities, with unprecedented spatial resolution and sensitivity, making them highly interesting for biomedical applications.

- Optically pumped magnetometers offer new functionalities in clinical magnetoencephalography, with their wearable sensor helmet allowing the subject to perform tasks and move during the recording of brain activity.

- Nitrogen–vacancy (NV)-centre-based magnetometry of single neurons and magnetic biomarkers, with subcellular resolution, opens new avenues in studying neuronal circuits and in rapid clinical testing.

- Nuclear magnetic resonance based on NV centres in diamond enables microscale and nanoscale detection of single molecules and single cells, which could be applied in structure determination of transmembrane proteins and in metabolomics studies.

- Nanodiamonds containing NV centres can locally probe temperature-dependent biological processes in cells and small organisms, such as cell development and endogenous heat generation.

Introduction

Advances in biomedical sciences are often spurred by the development of tools with enhanced sensitivity and resolution, which allow detection and imaging of signals that are progressively weaker, more localized and/or biologically specific. Improvements in nuclear magnetic resonance (NMR) or magnetoencephalography (MEG) have resulted in tremendous progress in diagnostics and treatment, yet further progress in sensitivity and resolution seems to be challenging with conventional methods. However, a promising direction for a new generation of biomedical sensors with greatly enhanced performance comes from advances in quantum science and technology.

Control and measurement of individual quantum systems, which seemed impossible only a few decades ago, is now a reality in many laboratories worldwide. This achievement has generated much excitement in both academia and industry. Quantum computation and quantum communication have garnered great attention[1–3], but quantum sensing, another pillar of quantum technology, is also advancing rapidly. One advantage of quantum sensors is the improvement in sensitivity that stems from quantum effects. Some quantum sensors are as small as a single atom and can consequently yield unmatched spatial resolution. These new capabilities could lead to a true 'quantum leap' in biomedical applications. First attempts have already been made, in the form of quantum-sensor-based brain imaging[4] and NMR at the scale of individual proteins and cells[5,6]. This is an exciting time for quantum sensing as it transitions from academic laboratories to commercial applications.

The focus of this Review is on two promising quantum platforms as exemplars of quantum sensors in biomedical applications: optically pumped magnetometers (OPMs) and magnetometry based on nitrogen–vacancy (NV) centres in diamond. An overview of the potential applications on the molecular, cellular and organism levels is given in Fig. 1. We present four case studies, chosen among the many

directions that are being actively explored. The first is MEG based on OPMs, with an emphasis on its advantages over conventional MEG based on superconducting quantum interference devices (SQUIDs). The second case study discusses how diamond sensor chips with an ensemble of NV centres can be used for magnetic sensing and microscopy of biological cells and tissue. The third is dedicated to NV-diamond sensing applied to nanoscale and microscale NMR imaging and spectroscopy. The final case study will discuss nanoscale thermometry with NV centres in nanodiamonds. For discussion of the principles of quantum sensing, we refer readers to other reviews[7–10].

What are quantum sensors?

Quantum sensors are individual systems or ensembles of systems that use quantum coherence, interference and entanglement to determine physical quantities of interest[7]. In what follows, we do not limit the discussion to entanglement-enhanced sensing, although there have been numerous early demonstrations of such capabilities in the field.

Quantum sensors have been realized in multiple systems with very different operating principles. This diversity makes them each suitable for different applications and allows them to be used in complementary ways. In the following, we give a brief overview of the most prominent examples of quantum sensors.

Superconducting circuits

One of the earliest quantum sensors is the SQUID. Based on superconducting Josephson junctions, SQUIDs can measure magnetic fields with sensitivities reaching 10 aT $Hz^{-1/2}$ in controlled laboratory settings[11]. Many SQUID sensors are commercially available and are, for example, applied in MEG, where they detect magnetic signals from the brain. However, SQUIDs require cryogenic operation, which necessitates bulky set-ups and limits the achievable spatial resolution for real-world applications.

Atomic ensembles

Alkali atom ensembles in vapour cells can be spin-polarized, and their magnetic field coupling can be probed through optical means (Fig. 2a). Besides the absorption-based approach described in Fig. 2a, magnetic field detection can also be achieved by measuring d.c. and a.c. polarization rotation of the probe light[8]. These OPMs can achieve minute-long coherence times[12] and magnetic field sensitivities of 100 aT $Hz^{-1/2}$ in the laboratory[13]. Spin-exchange relaxation-free OPMs are operated at elevated temperatures of 100 °C and near-zero magnetic field. The high temperature requires insulation from target samples, and the requirement for near-zero magnetic field necessitates additional coils to cancel out environmental magnetic fields. OPM cells have been miniaturized down to the millimetre scale, but with degradation in sensitivity, ultimately limiting the spatial resolution for a given sensitivity[14]. Entanglement-enhanced sensing has also been demonstrated with OPMs[15,16]. The combination of these properties has enabled OPM application in NMR[17], MEG[4], magnetocardiography (MCG)[18] and magnetic induction tomography[19,20].

Solid-state spins

Electronic spin defects in semiconductors can also be used for quantum sensing. Diamond stands out as a special host material for optically addressable defects, owing to its large bandgap. Most notably, the NV colour centre in diamond has been widely studied as a quantum sensor[21,22]. Optical initialization and readout of the spin state has been demonstrated down to the single-NV level[23] (Fig. 2b). Owing to low

Review article

spin–orbit coupling, the NV's ground-state spin can reach coherence times of ~1 ms under ambient conditions[24]. NV centres have been shown to function over large ranges of temperature (4 K to 625 K)[25], magnetic field (up to 8.3 T)[26] and pressure (up to 13.6 GPa)[27]. These properties make the NV and other colour centres in diamond[28] attractive not only for quantum sensing but also for quantum information processing[29] and quantum communication[3]. For magnetometry, the photon shot-noise-limited sensitivity can be enhanced by a factor of $1/\sqrt{N}$ by using an ensemble of N NV centres, with an experimentally achieved sensitivity of ~1 pT Hz$^{-1/2}$ (ref. [30]). In addition, NV centres can be used as a sensor for temperature[31], electric fields[32] and pressure[27].

NV centres exhibit a sensing bandwidth ranging from d.c. to gigahertz frequencies[33]. In wide-field imaging applications using NV ensembles, the spatial resolution is typically set by the diffraction limit of the optical microscope. However, by combining NVs with scanning techniques, such as atomic force microscopy, the spatial resolution can be improved to the few-nanometre level, mainly limited by the NV-to-surface distance[34]. It is also possible to create nanodiamonds containing NV centres, which can be functionalized and serve as local probes[31]. Other defects in diamond (such as silicon vacancy centres[28]) and defects in different host materials (such as silicon carbide[35] or yttrium orthosilicate[36]) are being actively investigated as quantum sensors. As yet, they do not show sensitivities comparable to the NV centres, owing to their limited coherence properties.

In this Review, we highlight biomedical applications of OPMs and diamond NV centres as an illustration of the broad operating regimes that quantum sensors can cover. The OPMs and NV centres have complementary strengths and weaknesses. The high sensitivity of OPMs makes them suitable for macroscopic detection of weak magnetic fields, such as those generated by the brain or the heart. Conversely, a major advantage of NV centres is the short sensor-to-sample distance, allowing high spatial resolution and high sensitivity to weak, microscopic signals. In addition, the NV centre is a multifunctional sensor (detecting a.c. and d.c. magnetic fields, temperature and so on) and operates under a wide range of conditions. This multifunctionality makes it attractive for spectroscopy and diagnostics on the cellular level.
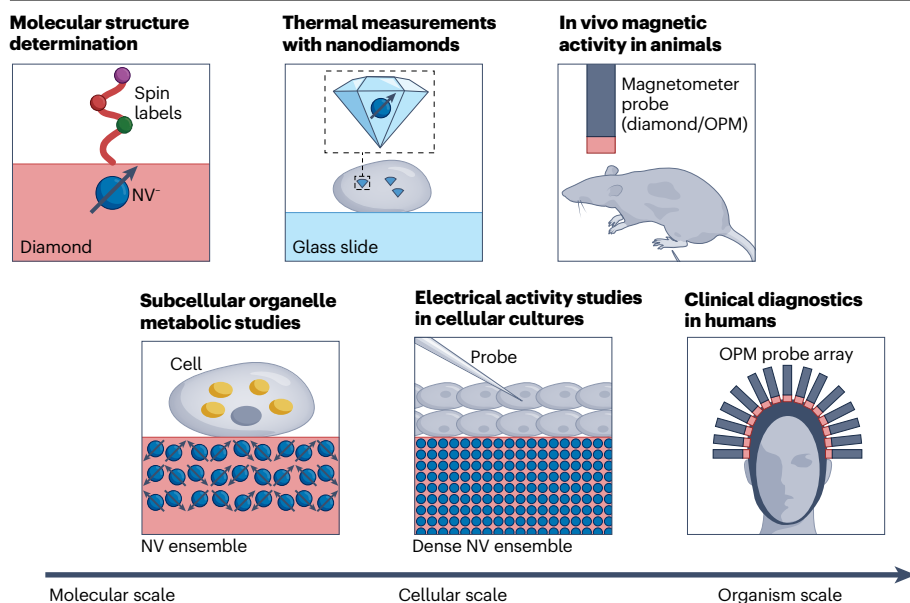
OPM-based MEG

Monitoring and imaging biomagnetism from the human body is useful for diagnostic and treatment purposes[37]. For example, the brain produces magnetic fields through the flow of electric currents in neurons. These fields are detected by MEG and can be used to study brain injury[38] and brain disorders such as epilepsy[39] and dementia[40].

Conventional MEG, as first demonstrated in the early 1970s, is based on SQUID sensors[41,42] and exhibits a noise level of fT Hz$^{-1/2}$. Despite considerable commercial and clinical adoption, the demanding operation conditions of MEG still pose severe limitations. For example, SQUID operation requires cryogenic temperatures, which makes the sensor array bulky (weighing over 400 kg for the helmet that holds the sensor array) and increases the sensor-to-subject distance. This distance not only limits signal-to-noise ratio and spatial resolution but also makes it infeasible for the subject to move during the recording. Moreover, the fixed MEG helmet's size complicates brain imaging because the subject's head profile can vary significantly, especially in the case of children.

The emergence of quantum sensing techniques has opened new avenues to tackle these limitations. Most promising are commercially available OPMs that can achieve sensitivities of ~10 fT Hz$^{-1/2}$ (ref. [43]), comparable to clinical SQUID devices. OPMs do not require low temperatures, thus simplifying the sensor architecture and allowing short sensor-to-sample distances. Another benefit of OPMs is their ability to detect vector magnetic fields[44–46], whereas SQUIDs only measure the magnetic field component radial to the scalp surface. Such tri-axial detection results in an overall higher signal strength and helps differentiate signal and background fields. Furthermore, progress in miniaturization of OPMs has enabled prototype OPM-MEGs to be built[4] (Fig. 3a), paving the way towards real-world applications.

To detect the weak magnetic signal originating from the brain, it is crucial to suppress much stronger magnetic-field backgrounds. Such suppression is achieved through magnetic shielding and fast field compensation with electromagnetic coils[47–50]. This approach, combined with the light weight (about 1 kg) of an OPM-MEG helmet, has enabled head movement up to 10 cm during human MEG recording[4].

Molecular structure determination

Spin labels

NV⁻

Diamond

Thermal measurements with nanodiamonds

Glass slide

In vivo magnetic activity in animals

Magnetometer probe (diamond/OPM)

Subcellular organelle metabolic studies

Cell

NV ensemble

Electrical activity studies in cellular cultures

Probe

Dense NV ensemble

Clinical diagnostics in humans

OPM probe array

Molecular scale → Cellular scale → Organism scale

Fig. 1 | Quantum sensors will have an impact in biomedical research on different length scales. Nitrogen–vacancy (NV) centres in diamond are suited for structure determination of single molecules. On the cellular scale, NV centres could help study metabolism and probe electrical activity of neurons. Such quantum sensors can also be integrated into nanodiamonds and serve as in vivo nanoscale temperature sensors. Detection of biomagnetic signal from animals and humans is another promising application of quantum sensors. In this regard, optically pumped magnetometers (OPM) are well suited due to their high magnetic field sensitivity.

Review article
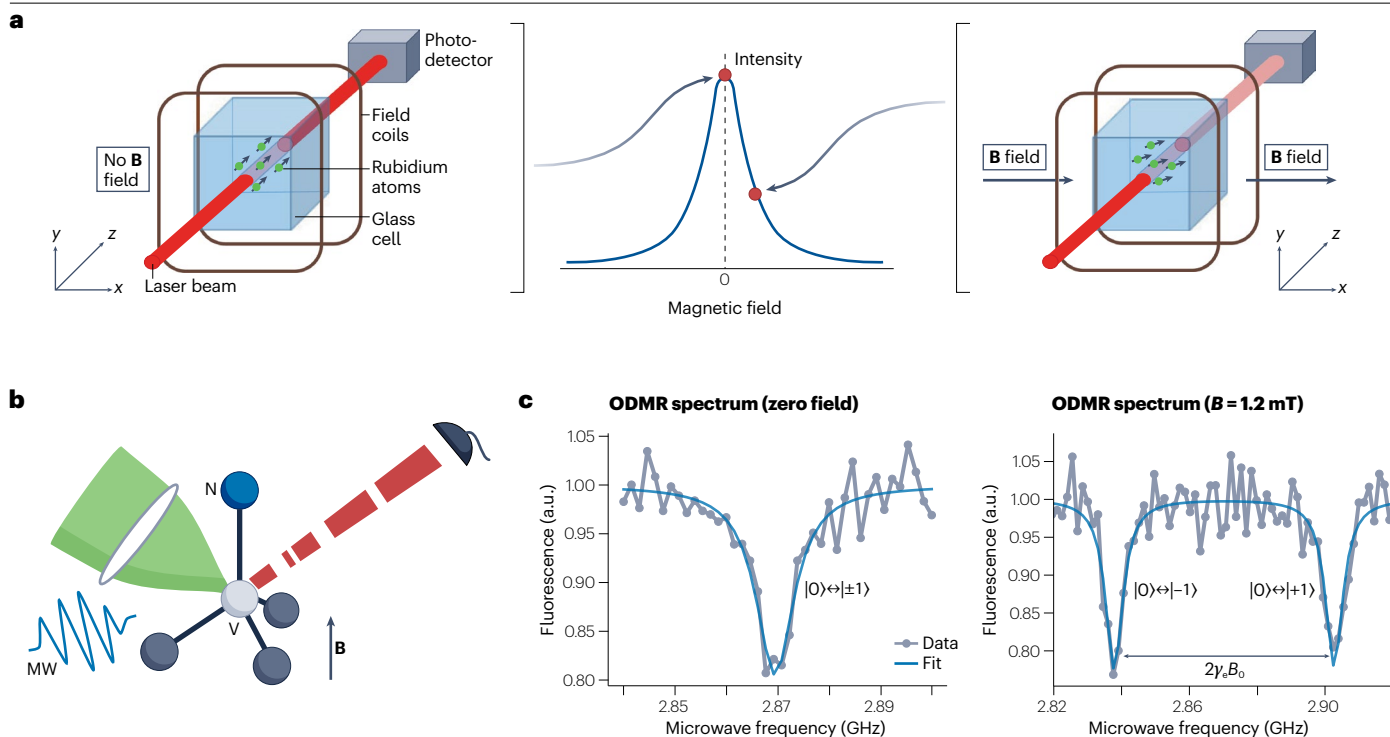
Fig. 2 | Operating principles of optically pumped magnetometers (OPMs) and nitrogen–vacancy (NV) magnetometers. a, In an OPM, rubidium atoms (as an example out of the various alkali atoms being used) in a glass cell are optically spin-polarized. In zero magnetic field, the transmission of a probe laser is at its maximum (left). The presence of a magnetic field leads to Larmor precession of the spins, which reduces transmission of the probe laser (right). **b**, The NV centre in the diamond lattice has its spin state initialized and interrogated via green excitation light, microwave (MW) resonant fields and red fluorescence, in the presence of magnetic fields (**B**). **c**, Optically detected magnetic resonance (ODMR) spectrum of the NV centre at zero field (left) and at $B = 1.2$ mT (right), where γ is the electron gyromagnetic ratio and $|0\rangle$, $|\pm1\rangle$ stand for the electron spin states $m_s = 0, \pm1$, respectively. Part **a** adapted with permission from ref. [4], Springer Nature Ltd.

It also allowed the subject to bounce a ball off a bat or to rotate their head while a MEG signal was recorded[4] (Fig. 3b). MEG detection has also been demonstrated at ambient conditions without magnetic shielding by combining two OPM magnetometers into a first-order gradiometer[51].

Another key advantage of OPMs not needing cryogenics is that the MEG helmet can be made to fit any head size (Fig. 3c). This possibility is especially helpful for neuroimaging of infants and enables long-term studies as the infants grow[52]. Subjects who are intimidated by the bulky SQUID-based MEG helmet, and others who cannot stay still during the imaging procedure, could also get access to MEG scans.

OPM-based MEGs are increasingly finding clinical application. OPMs have been applied to detect and localize focal interictal spikes in children with epilepsy[53] (Fig. 3d). For many neuroscientific studies it is also important to detect signal from deeper within the brain. One example is the human hippocampus, which is crucial for navigation and has been studied with OPM-based MEGs[54,55]. Another proof-of-concept demonstration has been the detection of functional connectivity with a 50-channel OPM[56], paving the way for studies of brain networks. Moreover, OPMs have successfully been used to measure human retinal activity[57]; the use of OPMs is contactless, in contrast to the fibre electrodes currently used. Another exciting demonstration of OPM-MEG has been the detection of human visual gamma-band activity in the brain[58]. These high-frequency oscillations are assumed to play an important role in

cognitive functions. The high spatial resolution of OPMs aids the localization of the active source areas, which is challenging with currently used techniques[58]. OPMs will also enable new possibilities in functional neuroimaging. For example, neuroscientists can now monitor brain activity while the subject moves and performs tasks of interest[4]. One can even envisage combining OPM-MEG with virtual-reality devices[59].

OPM-MEG is a relatively new technique, and further improvements are required before it can achieve widespread use in hospitals. Currently, the noise floor measured with OPMs is higher than SQUIDs by a factor of three, negating the sensitivity increase coming from smaller sensor-to-sample distance. So far, <100 OPM sensors have been combined into an array for MEG measurements[60] (https://www.cercamagnetics.com/cerca-opm-meg), in contrast to typical SQUID-MEG arrays of ~300 sensors. Scaling up the OPM sensor array, to provide comparable or superior resolution to SQUID-based MEG, will require the suppression of crosstalk between individual OPMs. The OPM community is working on these challenges and moving towards commercialization.

Another notable application of OPMs is MCG[18,51] (Fig. 3e). In this case, the measurement of magnetic fields from the heart allows diagnosis of diverse heart conditions associated with electrically active cardiac cells. The main advantages of OPM-MCG, relative to SQUID-based detectors, are its portability, low cost, and electrode-free application[61]. Some commercial OPM-MCG devices are already available (https://genetesis.com).

NV-based magnetic sensing and imaging of cells and tissues

Individual cells and tissues can produce magnetic fields, as exemplified by the fields produced by neuronal action potentials or by chains of magnetic nanoparticles (magnetosomes) in bacteria. Magnetic tags can also be introduced into living systems, in the form of magnetic nanoparticles (MNPs) or spin labels, for example. In all these cases, a biocompatible magnetometer with high sensitivity and high spatial resolution is required to measure the fields. One common method for such investigations uses a millimetre-scale diamond chip with a thin surface layer (micrometre scale) of ensemble NV centres[62]. Another commonly used modality is nanodiamonds containing NV centres, which can be injected or ingested into cells or tissues and functionalized, to target proteins of interest, for example.

Magnetic nanoparticle imaging

Labelling, detecting and targeting individual cells is useful for diagnostic applications, such as distinguishing cancer cells from healthy cells. Fluorescent markers are commonly used as labels, but often suffer from blinking, photobleaching and background autofluorescence.
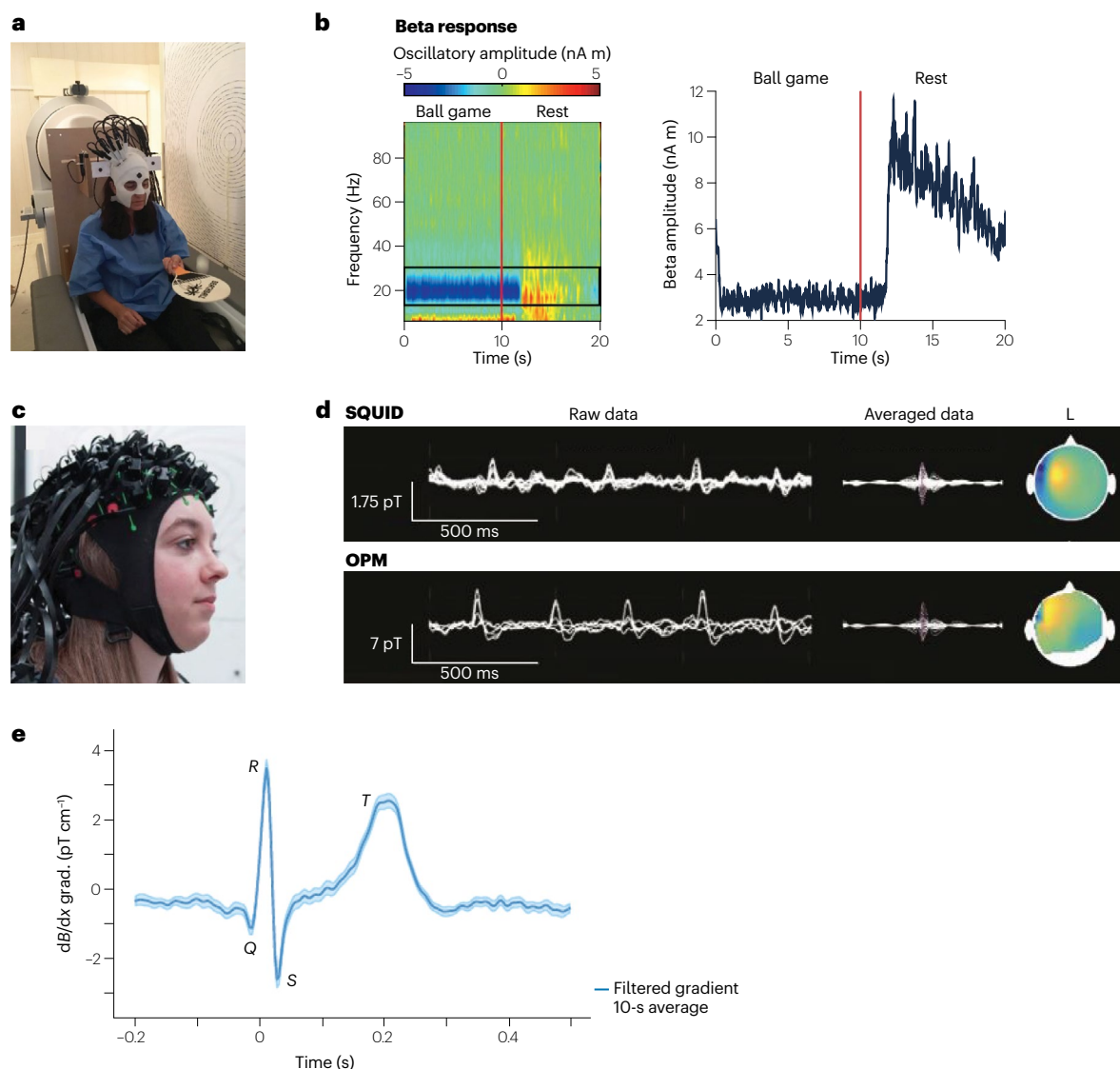
Fig. 3 | Optically pumped magnetometer (OPM)-based magnetoencephalography (MEG). a, Prototype wearable OPM-MEG. The subject can move their head during the measurement, as exemplified by the subject bouncing a tennis ball off a bat. **b**, Beta band oscillations recorded as a frequency spectrogram (left) and amplitude (right) during ball game and rest. **c**, Flexible wearable OPM-MEG helmet with 63 sensor mounts. **d**, SQUID-MEG (top) and OPM-MEG (bottom) recording of 11-year-old patient with refractory focal epilepsy. Left: superimposed data of multiple sensors showing filtered background brain activity and interictal epileptiform discharges (IEDs). Right: averaged IED data and magnetic field topography at the spike peak. **e**, OPM-magnetocardiography (MCG) measured at ambient conditions with a ^{87}Rb magnetic gradiometer. Parts **a**,**b** adapted with permission from ref. [4], Springer Nature Ltd. Part **c** adapted with permission from ref. [149] under a Creative Commons licence CC BY 4.0. Part **d** adapted with permission from ref. [53], RSNA. Part **e** adapted with permission from ref. [51], APS.

Review article

MNPs form the basis of magnetic immunoassay techniques, an emerging complementary diagnostic modality with potential advantages over fluorescent markers: long-term stability, negligible background signal and quantitative detection.

Diamond NV centres have been used for quantitative detection and wide-field imaging of MNPs in diverse biological samples, with micrometre-scale resolution and a millimetre field of view. In an early demonstration, NV-based magnetic microscopy was used to resolve and quantitatively characterize chains of MNPs (magnetosomes) that occur naturally in magnetotactic bacteria[62]. NV-based magnetic microscopy was also used to detect cancer biomarkers[63] (Fig. 4a,b). In this study, SKBR3 cancer cells were labelled with HER2-specific MNPs (where HER2 is human epidermal growth factor receptor 2), allowing differentiation between healthy and cancer cells. The technique is now commercially available for diagnostic assessment of biomarkers in human blood and other samples (https://qdti.com/). In another demonstration, NV-diamond magnetic microscopy was used to investigate malarial haemozoin nanocrystals, which serve as biomarkers for malaria[64] (Fig. 4c). These nanocrystals are formed in human blood cells infected by *Plasmodium falciparum*. In this study, the paramagnetic nature of the haemozoin nanocrystals was confirmed, and a magnetic susceptibility of 3.4×10^{-4} was measured, opening a possibility of drug screening against cells infected by *Plasmodium*.

In another demonstration, NV-based magnetic microscopy was applied to detect concentrations of magnetically labelled protein, interleukin-6[65], from patients hospitalized with COVID-19. Interleukin-6
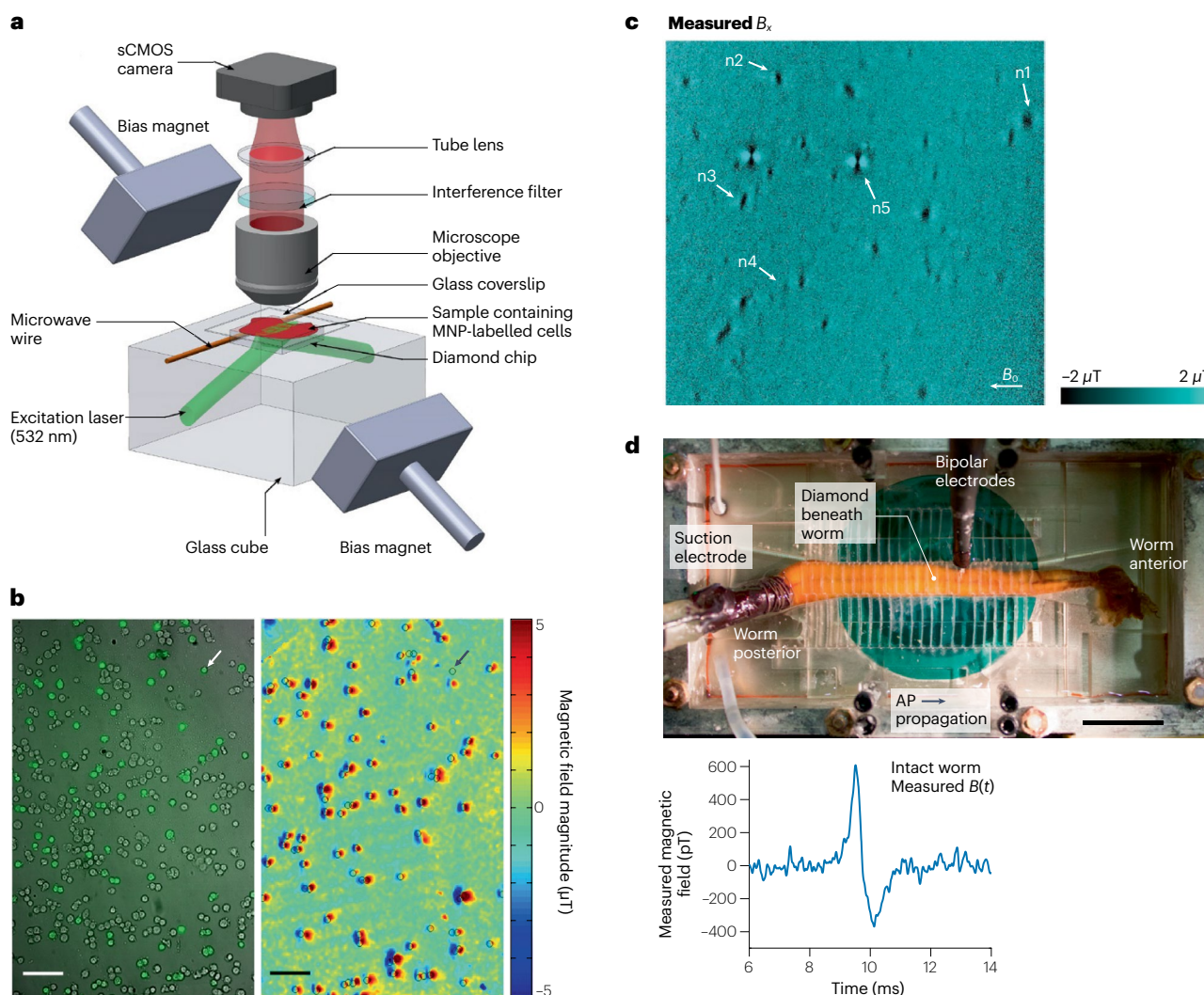
Fig. 4 | Nitrogen–vacancy (NV)-centre-based magnetic sensing of biological samples. a, Wide-field NV-diamond microscope for magnetic imaging of cells. sCMOS, scientific complementary metal–oxide–semiconductor. **b**, Wide-field imaging of biomarkers. Left: bright-field image overlaid with fluorescence image of SKBR3 cancer cells labelled with magnetic nanoparticles (MNPs) and stained with fluorescence dyes. Right: same field of view showing NV magnetic imaging of MNP-labelled cells. Scale bar, 100 μm. **c**, Magnetic field image of natural haemozoin crystals acquired with a NV-diamond microscope. Field of view is 39×39 μm². **d**, Top: image of NV-diamond set-up for single-neuron action potential (AP) magnetic measurement of a living specimen of *Myxicola infundibulum* (worm). Bottom: time trace of the magnetic field signal coming from a single-neuron action potential of *M. infundibulum* detected with the NV-diamond set-up. Part **a** adapted with permission from ref. [62], Springer Nature Ltd. Part **b** adapted with permission from ref. [63], Springer Nature Ltd. Part **c** adapted with permission from ref. [64] under a Creative Commons licence CC BY 4.0. Part **d** adapted with permission from ref. [66], PNAS.

Review article

is an endogenous cytokine associated with various diseases, such as severe COVID-19. The key idea was to detect the concentration of magnetic beads in the sample, and the results correlated well with the well-established Luminex assay technique. This success demonstrates the potential of NV-based microscopy for applications including rapid clinical testing.

Single-neuron action potential measurement

MEG is a powerful tool to investigate brain activity on macroscopic scales by interpreting effective current dipole sources in vivo. It would be desirable to understand how these effective current dipoles are related to underlying neuronal circuits. Such studies require minimally invasive magnetic measurements, ranging from single cells at the microscale to full neuronal circuits at the millimetre scale. NV-based microscopy has been used for a proof-of-concept measurement towards that direction. In this study, shallowly implanted diamond NV centres were used to measure the action potentials of single neurons from marine worms and squid[66] (Fig. 4d). The study achieved a magnetic field sensitivity of ~10 pT Hz$^{-1/2}$. Importantly, the submillisecond time resolution of the technique allowed the direct measurement of the action potential waveforms, including the direction of action potential propagation along the neuron and detection in whole, live animals. These studies at both the single-neuron and neuronal-circuit levels would improve and validate assumptions used in MEG for current dipole source reconstruction and could potentially improve the resolution of MEG as a result.

Detection of spin labels with T1 relaxometry

The measurement of the longitudinal relaxation time (T1) of NVs is sensitive to magnetic noise at the NV spin-transition frequency, from megahertz to the gigahertz regime. This method can be applied to enable highly sensitive detection of magnetic ions such as Gd^{3+}, the most common contrast agent used in magnetic resonance[67]. NV centres are allowing studies with these contrast agents down to the scale of individual cells, such as the detection and imaging of the plasma membrane of a HeLa cell labelled with Gd^{3+} ions, with a spatial resolution of 400 nm (ref. [68]). The resolution of NV T1 relaxometry can be further improved with a NV scanning probe set-up, as demonstrated by a spatial resolution of 10 nm for intracellular ferritin in Hep G2 cells[69].

Biomagnetic sensing with nanodiamonds

Bringing very small biological samples (such as organelles within cells) close to the NV centres located in a macroscopic diamond chip can be challenging. Nanodiamonds containing NV centres are being investigated as an alternative approach for such applications. Nanodiamonds can be inserted into the interior of cells, tissue and other biological samples. Functionalization of the nanodiamond surface can also enable targeting to proteins or other biological targets of interest. As the NV axis is randomly oriented for nanodiamonds, it is difficult to perform sensitive NV magnetometry using coherent techniques such as optically detected magnetic resonance (ODMR). However, NV T1 relaxometry can still be used, thus allowing the detection of metalloproteins[70], Gd^{3+} spin-labelled lipid bilayers[71] and the rotational Brownian motion of spin-labelled molecules[72].

A further application of T1 relaxometry with NV centres in nanodiamonds is the nanoscale detection of free radicals in biological samples. Formation of free radicals is linked to cardiovascular diseases and neurological disorder[73]. Free radicals can also play a vital role for the immune system[74]. Their sensitive detection with subcellular spatial resolution can therefore have far-reaching consequences in understanding biological processes. T1 relaxometry with NV centres in nanodiamonds makes such detection possible and has recently been used to study free radicals in single mitochondria[75] and in human dentritic cells[76]. In these experiments, the challenge is to carefully analyse the effect of free radicals on the T1 of the NV and rule out other influences. Another promising nanodiamond application is in vivo thermometry, which is discussed below.

Challenges and outlook

A key challenge for NV-based magnetic sensing and imaging of cells and tissues is to improve the sensitivity, which can lead to faster measurements and enable real-time mapping of neuronal activity and real-time functional imaging of biological samples, for example. Here we discuss some key opportunities for improved sensitivity[9]: improved readout techniques, which includes increasing the readout fidelity and minimizing the NV spin-state initialization and readout times; improved sample quality, which includes increasing the number of sensor spins per unit diamond sensing volume and extending the dephasing time; and improved measurement protocols, such as double quantum magnetometry[77].

Techniques to improve readout fidelity include spin-to-charge conversion[78], repetitive readout using nuclear spins coupled to the NV as quantum memories[79], and enhanced photon collection through various forms of diamond fabrication, tailored lenses or light guides[80]. Although these techniques have been highly successful for single NV measurements, more work is required for their adaptation to large-scale diamond chips with NV ensembles.

On the material side, high-density NV ensembles have typically been grown with high-pressure, high-temperature methods. More recently, high-quality chemical vapour deposition (CVD) samples have been prepared, including growth of thin nitrogen layers on relatively nitrogen-free substrates. To maximize NV creation in such layers, vacancy creation via electron irradiation is typically performed, resulting in NV ensembles with densities up to 4 ppm (ref. [81]). Unfortunately, the CVD growth process for high NV densities typically introduces additional paramagnetic defects and strain, affecting the coherence time of the sensor. Methods to mitigate these effects are being developed[82,83]. For NV centres within a few tens of nanometres of the diamond surface, surface-related charge instabilities and noise further degrade NV properties. Approaches to address this problem are actively being explored, including careful surface cleaning and termination[84], and delta doping of NVs, in which NVs are created in a thin surface layer and an additional diamond layer is then overgrown[85]. Another challenge in biomedical applications is reproducibility of results. To meet this challenge, it will be important to develop recipes to clean the diamond surface and maintain the coherence properties of the shallow NV centres in multiple rounds of experiments.

Nano- and microscale NMR with NV centres

NMR is a spectroscopic tool widely used in chemistry, biology and medicine for the structural determination of organic and biological molecules[86]. The technique usually relies on the detection of thermally polarized nuclear spins; to do so, large magnetic fields of the order of several tesla need to be applied[87,88]. A major limitation of traditional NMR is its low sensitivity, typically requiring millimetre-scale samples.

Extending NMR spectroscopy to microscale and nanoscale samples would enable exciting applications. It would, for example, allow chemical analysis of mass-limited samples that are expensive or

Review article

difficult to synthesize. Furthermore, NMR spectroscopy of a single-cell volume could enable detailed studies of cell structure and function, with applications in metabolomics and disease diagnosis[89,90]. Bringing NMR down to the nanometre scale would also make single-protein detection possible, opening up the possibility of determining the structure of functional membrane proteins under near-physiological conditions and studying their dynamics[91]. Membrane proteins are the targets of more than half of FDA-approved drugs[92], and the real-time study of protein–molecule binding would aid drug discovery.

NV-based NMR

The advent of NV-based magnetometry has enabled NMR spectroscopy of nanoscale and microscale samples under ambient conditions[6,93] (Fig. 5a). Here, the sample is placed near the NV centres in diamond, with distances in the range of nanometres to micrometres depending on the specific application[6,94] (Fig. 5a). At the nanoscale, NV-based NMR benefits from the large statistical polarization of the sample spins, while on the microscale, thermal polarization dominates[95], often necessitating further enhancements via high magnetic fields[96] and hyperpolarization methods[97,98]. One feature of NV centres is their large magnetic field sensing bandwidth, ranging from d.c. to gigahertz[7]. Detection of multiple nuclear spin species[99,100] and even electron spins[101] is therefore possible with the same experimental set-up, without the need of changing the radiofrequency equipment as is the case for traditional NMR and electron paramagnetic resonance spectroscopy.

Figures of merit

For NV-based NMR, the key figures of merit are the spatial resolution, spectral resolution and sensitivity of the spectrometer. The spatial resolution, or sensing volume, is of the order of the (depth)³ of the NV centres, typically ranging from $(4 \text{ nm})^3$ to $(10 \text{ μm})^3$, and can be chosen based on the specific application. For NV-ensemble measurements, the spatial resolution is further limited by the laser spot size. The sensitivity, conversely, follows similar considerations to those discussed in the previous section on NV-based magnetic sensing. At the nanoscale, single-proton spin detection in 1-s integration has been demonstrated[94]; whereas at the microscale, the detection of ~10^{14} thermally polarized proton spins (~10 picolitre) has been demonstrated with 1-s integration[6]. The sensitivity can be further improved via hyperpolarization, as discussed below.

To resolve molecule-specific resonances, such as chemical shifts and J-couplings, a high spectral resolution of around one part per million (of the order of hertz in absolute frequency units) is required[102]. This resolution has been realized using different techniques[5,6]. The achievable spectral resolution is limited by both the NV centre and the sample. The limitation from the NV centre depends on the applied sensing sequence: dynamical decoupling (Fig. 5b) can achieve a spectral resolution of ~1 kHz, limited by the NV T2 time[93]. Correlation spectroscopy can further improve the resolution to ~100 Hz, limited by the NV T1 time[99]. Even further enhanced spectral resolution can be reached with memory-spin-enhanced sensing[5,103], limited by the T1 of the NV nitrogen nuclear spin, which can be >260 s (ref. [103]). Another approach is to coherently average a sensing step that is then synchronized to an external clock[6,104,105] (Fig. 5c).

On the sample side, physical diffusion (liquids) or spin diffusion (solids) is often the limiting factor. Fast translational diffusion in liquids limits the spectral resolution to ~1 kHz for viscous liquids and makes liquids with low viscosity undetectable[100]. This problem can be addressed by confining samples into a nanoscale volume[106,107]. For

solid-state samples, dipole–dipole broadening is the limiting factor[94], and heteronuclear and homonuclear decoupling can help to improve the resolution[5]. Additionally, NV-based multidimensional NMR can help in reconstructing the chemical structure of a biomolecule. In a proof-of-principle experiment, 27 ^{13}C spins were localized in a diamond lattice relative to a single NV centre[108]. NV-based NMR has also been applied to samples external to the diamond, as demonstrated by the detection of a single protein with a spectral resolution of 1 kHz (ref. [94]).

Hyperpolarization

Spin polarization beyond thermal equilibrium, typically achieved by transferring polarization from more readily polarizable electronic spins to the target nuclear spins, can enhance the NMR signal and thus improve detection sensitivity. Dynamic nuclear polarization, based on the Overhauser mechanism[97], and parahydrogen-based signal amplification by reversible exchange (SABRE)[98] were used to hyperpolarize proton spins to 0.5%, leading to a signal enhancement of NV-based NMR of about 2×10^5 and the detection of target molecules at concentrations as low as 1 millimolar[98]. The NV spins can also serve as a source of hyperpolarization, because they can be well polarized via optical pumping (Fig. 2b). Through this technique, surrounding ^{13}C nuclear spins were polarized to ~720 times the thermal value at 7 T (refs. [109–111]). Unfortunately, no external spin hyperpolarization has yet been demonstrated. This is due to low diamond surface-to-volume ratios[111], decreased spin coherence times of near-surface NVs[112,113] and short nuclear spin T1 times close to the diamond surface[84,114]. Laboratories worldwide are working to address these challenges, by better control of the diamond surface and by achieving high densities of shallow NVs with improved coherence properties, for example[81,112,113].

Nanoscale and microscale magnetic resonance imaging

The full potential of NV-based NMR unfolds when imaging biological samples, as it can reveal changes in chemical composition at the nanoscale to microscale (Fig. 5d). At the microscale, magnetic resonance imaging (MRI) can be realized by a wide-field set-up with an ensemble of NV centres[100], and scanning probe systems can be used for MRI with higher spatial resolution of the order of ~10 nm (ref. [115]) (Fig. 5e).

Owing to the high sensitivity on the nanoscale of NV centres, NVs are also considered a promising tool for studying surface chemistry. Functionalization of the diamond surface is of great importance for these applications, because it immobilizes molecules close to NV centres and enables surface NMR detection with NV centres[116–118].

Future developments

It is well established that NV-based sensors can perform NMR spectroscopy of nanoscale and microscale samples and, under certain conditions, detect chemical shifts and J-couplings. Despite this progress, several major challenges remain for NV-based NMR. Incorporation into microfluidics is necessary for high-throughput NMR screening of certain samples, such as those that are mass-limited; higher sensitivities are required for structure determination of individual molecules; deterministic single (bio)molecule placement near a single NV centre would be desirable, possibly via scanning probe techniques[115] or surface treatment[116–118]; and finally, increased spectral resolution by reducing sample diffusion[106,107] and designing new pulse sequences[83] will be highly beneficial.

With these further developments, NV-based NMR will expand capabilities beyond conventional techniques and open many avenues
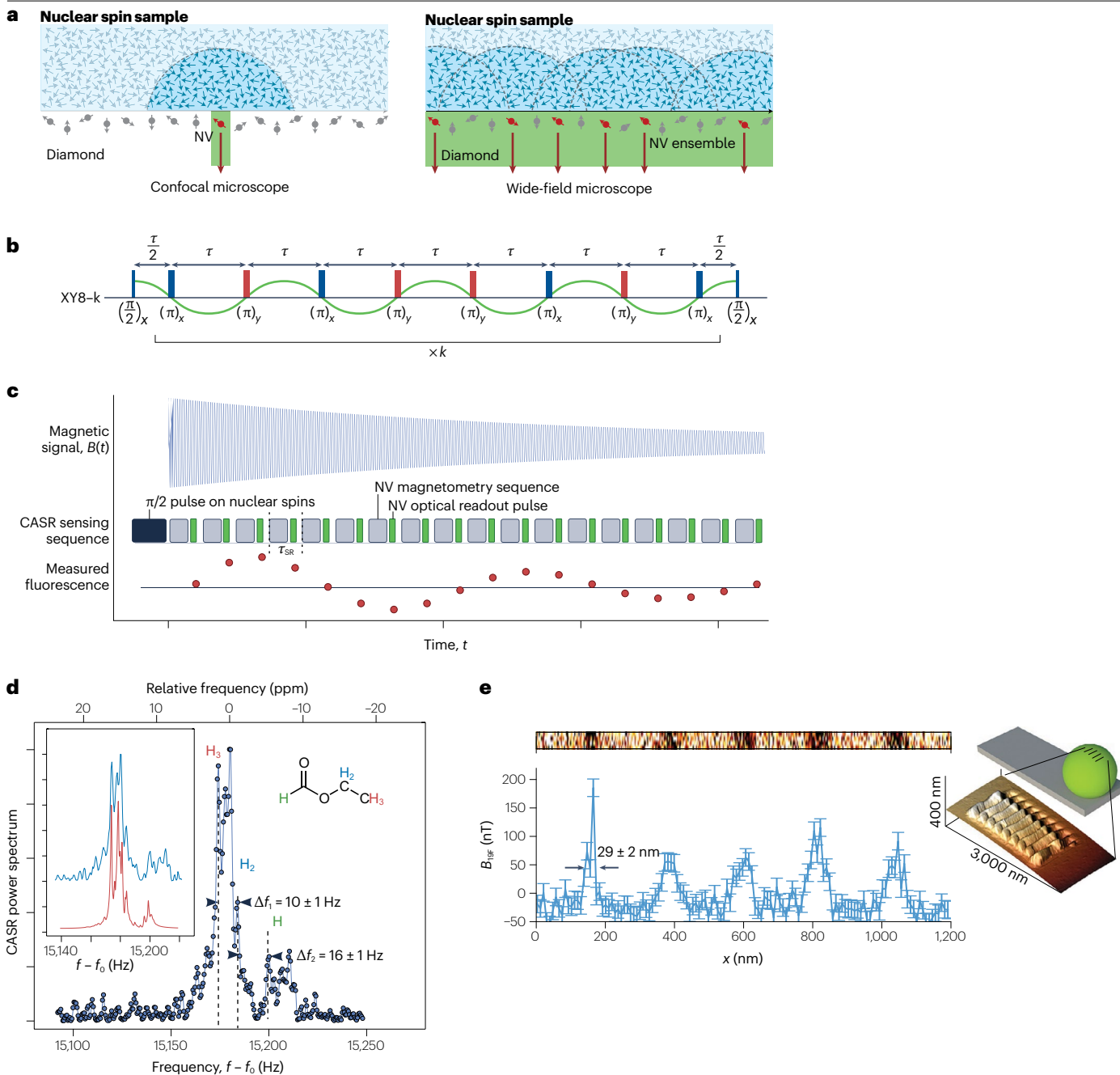
Fig. 5 | Nuclear magnetic resonance (NMR) with nitrogen–vacancy (NV) centres. a, Single-NV and NV-ensemble NMR set-ups. **b,c**, Pulse sequences used for NMR detection with NV centres: XY8-k (XY8 is a sequence of microwave pulses with X and Y phase shifts and is repeated k times, part **b**) and coherently averaged synchronized readout (CASR, part **c**). **d**, NMR spectrum detected by NV ensembles showing resolved chemical shift. **e**, Inset: image of a grating etched on a fluorine-enriched microsphere on an atomic force microscope tip. Main image: line scan of the NMR spectrum detected by a single NV centre as the sphere is moved over the NV centre. Parts **a,b** adapted with permission from ref. [100], Springer Nature Ltd. Parts **c,d** adapted with permission from ref. [6], Springer Nature Ltd. Part **e** adapted with permission from ref. [115], Springer Nature Ltd.

in chemistry as well as molecular and cell biology. Nanoscale NV-based NMR, aided by multidimensional spectroscopy and spin-labelling techniques, will enable the structural determination of complex molecules, such as transmembrane proteins in near-physiological conditions. Furthermore, wide-field NV-based MRI with its subcellular spatial resolution could be applied for single-cell metabolomics studies. Another application is to correlate NV-based NMR with optical microscopy of fluorophore labels, which can be useful for single-molecule studies. Ultimately, the goal would be to make these techniques accessible to non-physicists. Towards this goal, miniaturization of the tool

Review article

is important. With recent developments[119,120] and further integration, chip-scale NV spectrometers may become a reality soon.

NV thermometry

NV-based quantum thermometry

Whereas the preceding sections focused on applications to magnetic field sensing, quantum sensors can also be sensitive to a range of other environmental influences[10,27,28,31,32,121–125], providing rich sensing modalities relevant to the life sciences. In this section, we discuss one biological application of quantum sensors beyond magnetic field sensing: in vivo nanoscale thermometry with NVs in nanodiamonds. This modality enables local probing of a wide range of temperature-related biological phenomena in cells and small organisms, including the effects of external heat gradients and internal heat generation, providing tools for the control of cell cycles and organism development.

Like magnetic field sensing, NV-based quantum thermometry relies on temperature-dependent changes in microwave transition frequencies (Fig. 6a) that originate from thermal expansion of diamond. The vibronic interactions between the NV spin and the host lattice result in a temperature-dependent zero-field splitting[124], with a slope of approximately −74 kHz K^{-1} close to room temperature[31,121–124]. To optimize sensitivity while minimizing susceptibility to other effects, a four-point measurement scheme is typically used (Fig. 6b). The temperature can also be measured via purely optical means through changes in the emission spectrum and intensity[28,125], thus providing multimodal verification of results.

Nanodiamond quantum sensors are well suited for high-spatial-resolution temperature sensing in cells and small organisms. Compared with conventional temperature probes, nanodiamond quantum sensors are nanoscale, stable and biocompatible[126–129]. They also provide a complementary tool to luminescent nanoscale thermometry performed with fluorescent nanoparticles or proteins[130], which suffer from calibration issues, bleaching or susceptibility to frequency-dependent optical transmission[131]. Quantum sensing instead uses coherence between microwave transitions, reducing the sensitivity to optical transmission and other environmental factors.

NV centres can be created in nanodiamonds[10,31,70–72,127–129], often in the form of NV ensembles to further increase sensitivity. The size of such nanodiamonds is typically around 50–100 nm, although smaller

ones are available with inferior optical and spin properties[132]. With suitable surface treatment, these nanodiamonds can be delivered into individual cells. For some cell types, such as HeLa cells, natural uptake is sufficient, whereas for others, such as egg cells, injection techniques may be preferred[128,129]. Although suitably treated nanodiamonds have mostly been found to have no or low cytotoxicity, some studies suggest they can remain in organs for long periods[133], motivating further long-term studies of their effects[128,134]. The NV temperature sensitivity is ~5 mK Hz$^{-1/2}$ in isotopically purified, ultrapure bulk diamond[123]. The sensitivity in the nanodiamond form is poorer, however, because of strain effects and surface contamination. In a typical biological setting, the temperature sensitivity of NV nanodiamonds is ~1 K Hz$^{-1/2}$ (refs. [31,135–137]), comparable to other techniques[130].

Applications of nanoscale thermometry

Sensitive nanoscale thermometry opens many possibilities in life science applications, especially in combination with localized exogenous heating induced by infrared laser illumination (Fig. 6c). Laser heating has been used to explore the direct biochemical effects of elevated temperature (such as accelerated cell growth or protein denaturation)[31,135,138,139], the expression of heat-shock protein promoters[140–142], and thermal effects on cell and organism development. In an early proof-of-principle experiment that combines infrared heating and nanodiamond sensors, the threshold heating temperature that induces HeLa cell death was investigated[31]. More recently, local temperature manipulation and monitoring was used to control and invert the cell development cycle during embryogenesis in *Caenorhabditis elegans*[137]. Nanodiamonds have also been explored as a tool for in vivo temperature calibration for thermotherapeutic treatments[138,140]. Other possible applications of NV-based thermometry include nanoscale measurements of heat conductivity[143], and endogenous heat generation[135,144–146].

Challenges

Although current techniques have yielded impressive demonstrations and shed light on the role of temperature on biological processes, considerable challenges remain. First, to measure absolute temperature changes accurately, it is necessary to perform precise in vivo calibration of quantum sensors in the presence of internal strain, stray magnetic fields, spatial movement in cells, and microwave and optical heating.
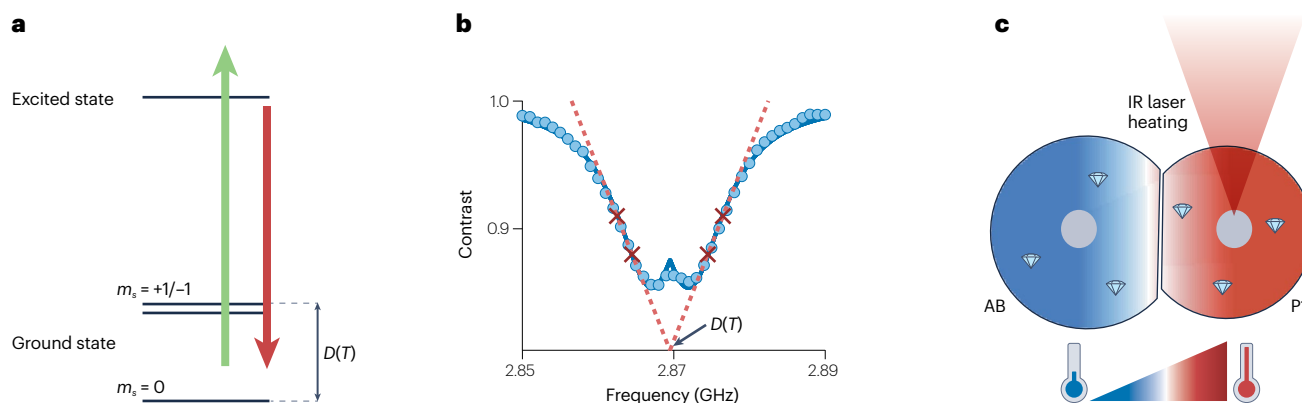
Fig. 6 | Thermometry with nitrogen–vacancy (NV) centres in nanodiamonds. **a**, NV energy-level diagram with spin quantum number m_s = 0,±1 and temperature-dependent zero-field splitting, $D(T)$, which is typically used for thermometry. **b**, Four-point measurement scheme for noise-robust determination of temperature using NVs. **c**, Heat gradients between two cells AB and P1 at the early embryo stage, generated by localized heating using an infrared (IR) laser. Parts **b,c** adapted with permission from ref. [137], PNAS.

Review article

Second, although techniques for incorporating nanodiamonds into living cells are fairly mature, more work is required on surface functionalization and nanodiamond synthesis to target specific organelles at the subcellular level[147]. Third, despite the fact that the temperature sensitivity of nanodiamond sensors is competitive with other technologies, further improvements are desired. These improvements include using hybrid nanodiamond–MNP schemes[148], material improvements, spin echo techniques for T2-limited NV coherence measurements[31,131,132] (instead of the current T2*-limited measurements) and advanced readout methods[9].

Outlook

The field of quantum sensors has developed tremendously in the past decade, moving from early proof-of-principle experiments into real-world applications in biomedical sciences. Indeed, these developments have already spurred the creation of several start-up companies making use of the technologies discussed in the case studies above. Examples (not exhaustive) include: QuSpin, CercaMagnetics and FieldLine Inc., focusing on commercializing OPM-MEG technology; ODMR Technologies, focusing on NV-based magnetic resonance spectroscopy for chemical trace analysis; Quantum Diamond Technologies Inc. (QDTI), focusing on wide-field NV magnetic imaging of disease biomarkers; and NVision Imaging Technologies, focusing on NV-based hyperpolarization of nuclear spins for molecular analysis and medical imaging.

Although there are promising opportunities, many challenges remain, probably calling for collaborations between multiple academic domains and industry. On the one hand, as discussed in the case studies for NV-based optical magnetic imaging and NMR spectroscopy, the sensitivities of current quantum sensors will probably need to be further improved through a combination of new sensing protocols and material developments. On the other hand, further integration and miniaturization of such technologies, to enable scalability and ease of operation under realistic conditions, will be crucial for broad acceptance and commercial success. With these improvements, we expect quantum sensors to become key tools for characterization and diagnostics of biomedical systems.

Published online: 3 February 2023

References

1. Arute, F. et al. Quantum supremacy using a programmable superconducting processor. *Nature* **574**, 505–510 (2019).
2. Zhong, H.-S. et al. Quantum computational advantage using photons. *Science* **370**, 1460–1463 (2020).
3. Bhaskar, M. K. et al. Experimental demonstration of memory-enhanced quantum communication. *Nature* **580**, 60–64 (2020).
4. Boto, E. et al. Moving magnetoencephalography towards real-world applications with a wearable system. *Nature* **555**, 657–661 (2018).
5. Aslam, N. et al. Nanoscale nuclear magnetic resonance with chemical resolution. *Science* **357**, 67–71 (2017).
6. Glenn, D. R. et al. High-resolution magnetic resonance spectroscopy using a solid-state spin sensor. *Nature* **555**, 351–354 (2018).
7. Degen, C. L., Reinhard, F. & Cappellaro, P. Quantum sensing. *Rev. Mod. Phys.* **89**, 035002 (2017).
8. Budker, D. & Romalis, M. Optical magnetometry. *Nat. Phys.* **3**, 227–234 (2007).
9. Barry, J. F. et al. Sensitivity optimization for NV-diamond magnetometry. *Rev. Mod. Phys.* **92**, 015004 (2020).
10. Schirhagl, R. et al. Nitrogen-vacancy centers in diamond: nanoscale sensors for physics and biology. *Annu. Rev. Phys. Chem.* **65**, 83–105 (2014).
11. Simmonds, M., Fertig, W. & Giffard, R. Performance of a resonant input SQUID amplifier system. *IEEE Trans. Magn.* **15**, 478–481 (1979).
12. Balabas, M. V. Polarized alkali-metal vapor with minute-long transverse spin-relaxation time. *Phys. Rev. Lett.* https://doi.org/10.1103/PhysRevLett.105.070801 (2010).
13. Dang, H. B., Maloof, A. C. & Romalis, M. V. Ultrahigh sensitivity magnetic field and magnetization measurements with an atomic magnetometer. *Appl. Phys. Lett.* **97**, 151110 (2010).
14. Shah, V. et al. Subpicotesla atomic magnetometry with a microfabricated vapour cell. *Nat. Photon.* **1**, 649–652 (2007).
15. Fernholz, T. et al. Spin squeezing of atomic ensembles via nuclear-electronic spin entanglement. *Phys. Rev. Lett.* **101**, 073601 (2008).
16. Wasilewski, W. et al. Quantum noise limited and entanglement-assisted magnetometry. *Phys. Rev. Lett.* **104**, 133601 (2010).
17. Xu, S. et al. Magnetic resonance imaging with an optical atomic magnetometer. *Proc. Natl Acad. Sci. USA* **103**, 12668–12671 (2006).
18. Jensen, K. et al. Magnetocardiography on an isolated animal heart with a room-temperature optically pumped magnetometer. *Sci. Rep.* **8**, 16218 (2018).
19. Deans, C. et al. Electromagnetic induction imaging with a radio-frequency atomic magnetometer. *Appl. Phys. Lett.* **108**, 103503 (2016).
20. Jensen, K. et al. Detection of low-conductivity objects using eddy current measurements with an optical magnetometer. *Phys. Rev. Res.* **1**, 033087 (2019).
21. Balasubramanian, G. et al. Nanoscale imaging magnetometry with diamond spins under ambient conditions. *Nature* **455**, 648–651 (2008).
22. Maze, J. R. et al. Nanoscale magnetic sensing with an individual electronic spin in diamond. *Nature* **455**, 644–647 (2008).
23. Gruber, A. et al. Scanning confocal optical microscopy and magnetic resonance on single defect centers. *Science* **276**, 2012–2014 (1997).
24. Balasubramanian, G. et al. Ultralong spin coherence time in isotopically engineered diamond. *Nat. Mater.* **8**, 383–387 (2009).
25. Toyli, D. M. et al. Measurement and control of single nitrogen-vacancy center spins above 600 K. *Phys. Rev. X* **2**, 031001 (2012).
26. Fortman, B. et al. Electron–electron double resonance detected NMR spectroscopy using ensemble NV centers at 230 GHz and 8.3T. *J. Appl. Phys.* **130**, 083901 (2021).
27. Hsieh, S. et al. Imaging stress and magnetism at high pressures using a nanoscale quantum sensor. *Science* **366**, 1349–1354 (2019).
28. Nguyen, C. T. et al. All-optical nanoscale thermometry with silicon-vacancy centers in diamond. *Appl. Phys. Lett.* **112**, 203102 (2018).
29. Bradley, C. E. et al. A ten-qubit solid-state spin register with quantum memory up to one minute. *Phys. Rev. X* **9**, 031045 (2019).
30. Zhang, C. et al. Diamond magnetometry and gradiometry towards subpicotesla DC field measurement. *Phys. Rev. Appl.* **15**, 064075 (2021).
31. Kucsko, G. et al. Nanometre-scale thermometry in a living cell. *Nature* **500**, 54–58 (2013).
32. Dolde, F. et al. Electric-field sensing using single diamond spins. *Nat. Phys.* **7**, 459–463 (2011).
33. Schäfer-Nolte, E. et al. Tracking temperature-dependent relaxation times of ferritin nanomagnets with a wideband quantum spectrometer. *Phys. Rev. Lett.* **113**, 217204 (2014).
34. Maletinsky, P. et al. A robust scanning diamond sensor for nanoscale imaging with single nitrogen-vacancy centres. *Nat. Nanotechnol.* **7**, 320–324 (2012).
35. Koehl, W. F. et al. Room temperature coherent control of defect spin qubits in silicon carbide. *Nature* **479**, 84–87 (2011).
36. Kornher, T. et al. Sensing individual nuclear spins with a single rare-earth electron spin. *Phys. Rev. Lett.* **124**, 170402 (2020).
37. Williamson, S. J. & Manfried H. *Advances in Biomagnetism* (eds Williamson, S. J. et al.) (Springer, 2012).
38. Allen, C. M. et al. Magnetoencephalography abnormalities in adult mild traumatic brain injury: a systematic review. *NeuroImage Clin.* **31**, 102697 (2021).
39. Poghosyan, V., Rampp, S. & Wang, Z. I. Editorial: magnetoencephalography (MEG) in epilepsy and neurosurgery. *Front. Human Neurosci.* https://doi.org/10.3389/fnhum.2022.873153 (2022).
40. Hughes, L. E. et al. Magnetoencephalography insights to dementia and drug intervention. *Alzheimer's Dement.* **17**, e052536 (2021).
41. Cohen, D. Magnetoencephalography: detection of the brain's electrical activity with a superconducting magnetometer. *Science* **175**, 664–666 (1972).
42. Hämäläinen, M. et al. Magnetoencephalography — theory, instrumentation, and applications to noninvasive studies of the working human brain. *Rev. Mod. Phys.* **65**, 413–497 (1993).
43. QZFM Gen-3. *QUSPIN* https://quspin.com/products-qzfm/.
44. Rea, M. et al. A 90-channel triaxial magnetoencephalography system using optically pumped magnetometers. *Ann. NY Acad. Sci.* **1517**, 107–124 (2022).
45. Brookes, M. J. et al. Theoretical advantages of a triaxial optically pumped magnetometer magnetoencephalography system. *NeuroImage* **236**, 118025 (2021).
46. Boto, E. et al. Triaxial detection of the neuromagnetic field using optically-pumped magnetometry: feasibility and application in children. *NeuroImage* **252**, 119027 (2022).
47. Rea, M. et al. Precision magnetic field modelling and control for wearable magnetoencephalography. *NeuroImage* **241**, 118401 (2021).
48. Iivanainen, J. et al. On-scalp MEG system utilizing an actively shielded array of optically-pumped magnetometers. *NeuroImage* **194**, 244–258 (2019).
49. Mäkinen, A. J. et al. Magnetic-field modeling with surface currents. Part I. Physical and computational principles of bfieldtools. *J. Appl. Phys.* **128**, 063906 (2020).
50. Holmes, N. et al. A bi-planar coil system for nulling background magnetic fields in scalp mounted magnetoencephalography. *NeuroImage* **181**, 760–774 (2018).
51. Limes, M. E. et al. Portable magnetometry for detection of biomagnetism in ambient environments. *Phys. Rev. Appl.* **14**, 011002 (2020).
52. Hill, R. M. et al. A tool for functional brain imaging with lifespan compliance. *Nat. Commun.* **10**, 4785 (2019).

53. Feys, O. et al. On-scalp optically pumped magnetometers versus cryogenic magnetoencephalography for diagnostic evaluation of epilepsy in school-aged children. *Radiology* **304**, 429–434 (2022).

54. Barry, D. N. et al.Imaging the human hippocampus with optically-pumped magnetoencephalography. *NeuroImage* **203**, 116192 (2019).

55. Tierney, T. M. et al. Mouth magnetoencephalography: a unique perspective on the human hippocampus. *NeuroImage* **225**, 117443 (2021).

56. Boto, E. et al. Measuring functional connectivity with wearable MEG. *NeuroImage* **230**, 117815 (2021).

57. Westner, B. U. et al. Contactless measurements of retinal activity using optically pumped magnetometers. *NeuroImage* **243**, 118528 (2021).

58. Iivanainen, J., Zetter, R. & Parkkonen, L. Potential of on-scalp MEG: robust detection of human visual gamma-band responses. *Hum. Brain Mapp.* **41**, 150–161 (2020).

59. Roberts, G. et al. Towards OPM-MEG in a virtual reality environment. *NeuroImage* **199**, 408–417 (2019).

60. Hill, R. M. et al. Multi-channel whole-head OPM-MEG: Helmet design and a comparison with a conventional system. *NeuroImage* **219**, 116995 (2020).

61. Batie, M. et al. Detection of fetal arrhythmia using optically-pumped magnetometers. *JACC Clin. Electrophysiol.* **4**, 284–287 (2018).

62. Le Sage, D. et al. Optical magnetic imaging of living cells. *Nature* **496**, 486–489 (2013).

63. Glenn, D. R. et al. Single-cell magnetic imaging using a quantum diamond microscope. *Nat. Methods* **12**, 736–738 (2015).

64. Fescenko, I. et al. Diamond magnetic microscopy of malarial hemozoin nanocrystals. *Phys. Rev. Appl.* **11**, 034029 (2019).

65. Atallah, J. et al. Rapid quantum magnetic IL-6 point-of-care assay in patients hospitalized with COVID-19. *Diagnostics* **12**, 1164 (2022).

66. Barry, J. F. et al. Optical magnetic detection of single-neuron action potentials using quantum defects in diamond. *Proc. Natl Acad. Sci. USA* **113**, 14133–14138 (2016).

67. Lauffer, R. B. Paramagnetic metal complexes as water proton relaxation agents for NMR imaging: theory and design. *Chem. Rev.* **87**, 901–927 (1987).

68. Steinert, S. et al. Magnetic spin imaging under ambient conditions with sub-cellular resolution. *Nat. Commun.* **4**, 1607 (2013).

69. Wang, P. et al. Nanoscale magnetic imaging of ferritins in a single cell. *Sci. Adv.* **5**, eaau8038 (2019).

70. Ermakova, A. et al. Detection of a few metallo-protein molecules using color centers in nanodiamonds. *Nano Lett.* **13**, 3305–3309 (2013).

71. Kaufmann, S. et al. Detection of atomic spin labels in a lipid bilayer using a single-spin nanodiamond probe. *Proc. Natl Acad. Sci. USA* **110**, 10894–10898 (2013).

72. Li, C. et al. All-optical quantum sensing of rotational Brownian motion of magnetic molecules. *Nano Lett.* **19**, 7342–7348 (2019).

73. Lobo, V. et al. Free radicals, antioxidants and functional foods: impact on human health. *Pharmacogn. Rev.* **4**, 118–126 (2010).

74. Knight, J. A. Review: free radicals, antioxidants, and the immune system. *Ann. Clin. Lab. Sci.* **30**, 145–158 (2000).

75. Nie, L. et al. Quantum monitoring of cellular metabolic activities in single mitochondria. *Sci. Adv.* **7**, eabf0573 (2021).

76. Nie, L. et al. Quantum sensing of free radicals in primary human dendritic cells. *Nano Lett.* **22**, 1818–1825 (2022).

77. Mamin, H. J. et al. Multipulse double-quantum magnetometry with near-surface nitrogen-vacancy centers. *Phys. Rev. Lett.* **113**, 030803 (2014).

78. Shields, B. J. et al. Efficient readout of a single spin state in diamond via spin-to-charge conversion. *Phys. Rev. Lett.* **114**, 136402 (2015).

79. Arunkumar, N. et al. Quantum logic enhanced sensing in solid-state spin ensembles. Preprint at https://arxiv.org/abs/2203.12501 (2022).

80. Babinec, T. M. et al. A diamond nanowire single-photon source. *Nat. Nanotechnol.* **5**, 195–199 (2010).

81. Edmonds, A. M. et al. Generation of nitrogen-vacancy ensembles in diamond for quantum sensors: optimization and scalability of CVD processes. Preprint at https://arxiv.org/abs/2004.01746 (2020).

82. Joos, M. et al. Protecting qubit coherence by spectrally engineered driving of the spin environment. Preprint at https://arxiv.org/abs/2101.09654 (2021).

83. Zhou, H. et al. Quantum metrology with strongly interacting spin systems. *Phys. Rev. X* **10**, 031003 (2020).

84. Sangtawesin, S. et al. Origins of diamond surface noise probed by correlating single-spin measurements with surface spectroscopy. *Phys. Rev. X* **9**, 031052 (2019).

85. Ohno, K. et al. Engineering shallow spins in diamond with nitrogen delta-doping. *Appl. Phys. Lett.* **101**, 082413 (2012).

86. Mansfield, P. Snapshot magnetic resonance imaging (Nobel Lecture). *Angew. Chem. Int. Ed.* **43**, 5456–5464 (2004).

87. Glover, P. & Mansfield, S. P. Limits to magnetic resonance microscopy. *Rep. Prog. Phys.* **65**, 1489 (2002).

88. Abraham, R., Fisher, J. & Loftus, P. *Introduction to NMR Spectroscopy* (Wiley, 2022); https://www.wiley.com/en-gb/Introduction+to+NMR+Spectroscopy-p-9780471918943.

89. Weisman, I. D. et al. Recognition of cancer in vivo by nuclear magnetic resonance. *Science* **178**, 1288–1290 (1972).

90. Lauterbur, P. C. Image formation by induced local interactions: examples employing nuclear magnetic resonance. *Nature* **242**, 190–191 (1973).

91. Fox, R. O., Evans, P. A. & Dobson, C. M. Multiple conformations of a protein demonstrated by magnetization transfer NMR spectroscopy. *Nature* **320**, 192–194 (1986).

92. Moraes, I. et al. Membrane protein structure determination — the next generation. *Biochim. Biophys. Acta* **1838**, 78–87 (2014).

93. Staudacher, T. et al. Nuclear magnetic resonance spectroscopy on a (5-nanometer) 3 sample volume. *Science* **339**, 561–563 (2013).

94. Lovchinsky, I. et al. Nuclear magnetic resonance detection and spectroscopy of single proteins using quantum logic. *Science* **351**, 836–841 (2016).

95. Herzog, B. E. et al. Boundary between the thermal and statistical polarization regimes in a nuclear spin ensemble. *Appl. Phys. Lett.* **105**, 043112 (2014).

96. Smits, J. et al. Two-dimensional nuclear magnetic resonance spectroscopy with a microfluidic diamond quantum sensor. *Sci. Adv.* **5**, eaaw7895 (2019).

97. Bucher, D. B. et al. Hyperpolarization-enhanced NMR spectroscopy with femtomole sensitivity using quantum defects in diamond. *Phys. Rev. X* **10**, 021053 (2020).

98. Arunkumar, N. et al. Micron-scale NV-NMR spectroscopy with signal amplification by reversible exchange. *PRX Quantum* **2**, 010305 (2021).

99. Lovchinsky, I. et al. Magnetic resonance spectroscopy of an atomically thin material using a single-spin qubit. *Science* **355**, 503–507 (2017).

100. DeVience, S. J. et al. Nanoscale NMR spectroscopy and imaging of multiple nuclear species. *Nat. Nanotechnol.* **10**, 129–134 (2015).

101. Schlipf, L. et al. A molecular quantum spin network controlled by a single qubit. *Sci. Adv.* **3**, e1701116 (2017).

102. Schwartz, I. et al. Blueprint for nanoscale NMR. *Sci. Rep.* **9**, 6938 (2019).

103. Pfender, M. et al. Nonvolatile nuclear spin memory enables sensor-unlimited nanoscale spectroscopy of small spin clusters. *Nat. Commun.* **8**, 834 (2017).

104. Boss, J. M. et al. Quantum sensing with arbitrary frequency resolution. *Science* **356**, 837–840 (2017).

105. Schmitt, S. et al. Submillihertz magnetic spectroscopy performed with a nanoscale quantum sensor. *Science* **356**, 832–837 (2017).

106. Cohen, D. et al. Confined Nano-NMR spectroscopy using NV centers. *Adv. Quantum Technol.* **3**, 2000019 (2020).

107. Aslam, N. et al. Nanoscale nuclear magnetic resonance with quantum sensors enhanced by nanostructures. In *Quantum 2.0 Conference and Exhibition (2022)* Paper QW4C.3 (Optica Publishing Group, 2022).

108. Abobeih, M. H. et al. Atomic-scale imaging of a 27-nuclear-spin cluster using a quantum sensor. *Nature* **576**, 411–415 (2019).

109. Ajoy, A. et al. Room temperature 'optical nanodiamond hyperpolarizer': physics, design, and operation. *Rev. Sci. Instrum.* **91**, 023106 (2020).

110. Ajoy, A. et al. Orientation-independent room temperature optical ^{13}C hyperpolarization in powdered diamond. *Sci. Adv.* **4**, eaar5492 (2018).

111. Schwartz, I. et al. Robust optical polarization of nuclear spin baths using Hamiltonian engineering of nitrogen-vacancy center quantum dynamics. *Sci. Adv.* **4**, eaat8978 (2018).

112. Tetienne, J.-P. et al. Spin properties of dense near-surface ensembles of nitrogen-vacancy centers in diamond. *Phys. Rev. B* **97**, 085402 (2018).

113. Rubinas, O. R. et al. Optimization of the coherence properties of diamond samples with an intermediate concentration of NV centers. *Results Phys.* **21**, 103845 (2021).

114. Dhomkar, S. et al. Charge dynamics in near-surface, variable-density ensembles of nitrogen-vacancy centers in diamond. *Nano Lett.* **18**, 4046–4052 (2018).

115. Häberle, T. et al. Nanoscale nuclear magnetic imaging with chemical contrast. *Nat. Nanotechnol.* **10**, 125–128 (2015).

116. Liu, K. S. et al. Surface NMR using quantum sensors in diamond. *Proc. Natl Acad. Sci. USA* **119**, e2111607119 (2022).

117. Xie, M. et al. Biocompatible surface functionalization architecture for a diamond quantum sensor. *Proc. Natl Acad. Sci. USA* **119**, e2114186119 (2022).

118. Abendroth, J. M. et al. Single-nitrogen–vacancy NMR of amine-functionalized diamond surfaces. *Nano Lett.* **22**, 7294–7303 (2022).

119. Stürner, F. M. et al. Integrated and portable magnetometer based on nitrogen-vacancy ensembles in diamond. *Adv. Quantum Technol.* **4**, 2000111 (2021).

120. Ibrahim, M. I. et al. High-scalability CMOS quantum magnetometer with spin-state excitation and detection of diamond color centers. *IEEE J. Solid State Circuits* **56**, 1001–1014 (2021).

121. Sotoma, S., Epperla, C. P. & Chang, H.-C. Diamond nanothermometry. *ChemNanoMat* **4**, 15–27 (2018).

122. Toyli, D. M. et al. Fluorescence thermometry enhanced by the quantum coherence of single spins in diamond. *Proc. Natl Acad. Sci. USA* **110**, 8417–8421 (2013).

123. Neumann, P. et al. High-precision nanoscale temperature sensing using single defects in diamond. *Nano Lett.* **13**, 2738–2742 (2013).

124. Acosta, V. M. et al. Temperature dependence of the nitrogen-vacancy magnetic resonance in diamond. *Phys. Rev. Lett.* **104**, 070801 (2010).

125. Plakhotnik, T. et al. All-optical thermometry and thermal properties of the optically detected spin resonances of the NV⁻ center in nanodiamond. *Nano Lett.* **14**, 4989–4996 (2014).

126. Mochalin, V. N. et al. The properties and applications of nanodiamonds. *Nat. Nanotechnol.* **7**, 11–23 (2012).

127. McGuinness, L. P. et al. Quantum measurement and orientation tracking of fluorescent nanodiamonds inside living cells. *Nat. Nanotechnol.* **6**, 358–363 (2011).

128. van der Laan, K. J. et al. Nanodiamonds for in vivo applications. *Small* **14**, 1703838 (2018).

129. Mohan, N. et al. In vivo imaging and toxicity assessments of fluorescent nanodiamonds in *Caenorhabditis elegans*. *Nano Lett.* **10**, 3692–3699 (2010).

Review article

130. Jaque, D. & Vetrone, F. Luminescence nanothermometry. *Nanoscale* **4**, 4301–4326 (2012).
131. Zhou, J. et al. Advances and challenges for fluorescence nanothermometry. *Nat. Methods* **17**, 967–980 (2020).
132. Smith, B. R. et al. Five-nanometer diamond with luminescent nitrogen-vacancy defect centers. *Small* **5**, 1649–1653 (2009).
133. Yuan, Y. et al. Biodistribution and fate of nanodiamonds in vivo. *Diam. Relat. Mater.* **18**, 95–100 (2009).
134. Wu, Y. et al. Diamond quantum devices in biology. *Angew. Chem. Int. Ed.* **55**, 6586–6598 (2016).
135. Fujiwara, M. et al. Real-time nanodiamond thermometry probing in vivo thermogenic responses. *Sci. Adv.* **6**, eaba9636 (2020).
136. Simpson, D. A. et al. Non-neurotoxic nanodiamond probes for intraneuronal temperature mapping. *ACS Nano* **11**, 12077–12086 (2017).
137. Choi, J. et al. Probing and manipulating embryogenesis via nanoscale thermometry and temperature control. *Proc. Natl Acad. Sci. USA* **117**, 14636–14641 (2020).
138. Jaque, D. et al. Nanoparticles for photothermal therapies. *Nanoscale* **6**, 9494–9530 (2014).
139. Lal, S., Clare, S. E. & Halas, N. J. Nanoshell-enabled photothermal cancer therapy: impending clinical impact. *Acc. Chem. Res.* **41**, 1842–1851 (2008).
140. Kamei, Y. et al. Infrared laser-mediated gene induction in targeted single cells in vivo. *Nat. Methods* **6**, 79–81 (2009).
141. Bath, D. E. et al. FlyMAD: rapid thermogenetic control of neuronal activity in freely walking Drosophila. *Nat. Methods* **11**, 756–762 (2014).
142. Hirsch, S. M. et al. FLIRT: fast local infrared thermogenetics for subcellular control of protein function. *Nat. Methods* **15**, 921–923 (2018).
143. Bastos, A. R. N. et al. Thermal properties of lipid bilayers determined using upconversion nanothermometry. *Adv. Funct. Mater.* **29**, 1905474 (2019).
144. Arai, S. et al. Mitochondria-targeted fluorescent thermometer monitors intracellular temperature gradient. *Chem. Commun.* **51**, 8044–8047 (2015).
145. Kiyonaka, S. et al. Genetically encoded fluorescent thermosensors visualize subcellular thermoregulation in living cells. *Nat. Methods* **10**, 1232–1238 (2013).
146. Baffou, G. et al. A critique of methods for temperature imaging in single cells. *Nat. Methods* **11**, 899–901 (2014).
147. Nagl, A., Hemelaar, S. R. & Schirhagl, R. Improving surface and defect center chemistry of fluorescent nanodiamonds for imaging purposes — a review. *Anal. Bioanal. Chem.* **407**, 7521–7536 (2015).
148. Wang, N. et al. Magnetic criticality enhanced hybrid nanodiamond thermometer under ambient conditions. *Phys. Rev. X* **8**, 011042 (2018).
149. Brookes, M. J. et al. Magnetoencephalography with optically pumped magnetometers (OPM-MEG): the next generation of functional neuroimaging. *Trends Neurosci.* **45**, 621–634 (2022).

Additional information
Correspondence should be addressed to Hongkun Park.